Article

Spectroscopic Characterization of the Exopolysaccharide of *Xanthomonas axonopodis* pv. *citri* in Cu²⁺ Resistance Mechanism

Denise Osiro,[a,b] Roberto W. Assis Franco[a] and Luiz Alberto Colnago,[a]*

[a]Embrapa Instrumentação Agropecuária, 13560-970 São Carlos-SP, Brazil

[b]Instituto de Química de São Carlos, Universidade de São Paulo, 13560-970 São Carlos-SP, Brazil

Analizou-se o papel do exopolissacarídeo (EPS) no mecanismo de resistência ao Cu²⁺ da *Xanthomonas axonopodis* pv. *citri* (*Xac)* com as espectroscopias de infravermelho com transformada de Fourier (FTIR), ressonância paramagnética eletrônica (RPE) e ressonância magnética nuclear (RMN). Os dados de FTIR demonstraram que as células cultivadas na presença de 0.2 mmol L⁻¹ de CuSO₄ produziram uma maior quantidade de exopolissacarídeo piruvatado do que as células cultivadas na sua ausência. Os dados de RPE indicaram que a quantidade de íons Cu²⁺ diminuiu com o tempo de cultura. Os dados de RMN de ¹³C mostraram a complexação dos íons de Cu²⁺ com o EPS. Esses resultados mostraram que o EPS tem um papel importante no mecanismo de proteção da *Xac* ao Cu²⁺ e este age no mecanismo inicial de proteção, ligando-se aos íons de Cu²⁺ livres, reduzindo sua difusão e o transporte ativo ao citoplasma . O Cu²⁺ também induz a produção de EPS piruvatado, que aumenta a capacidade de coleta e complexação desses íons.

We analyzed the role of exopolysaccharide in the *Xanthomonas axonopodis* pv. *citri* (*Xac*) Cu²⁺ resistance mechanism by Fourier transform infrared (FTIR), electron paramagnetic resonance (EPR) and nuclear magnetic resonance (NMR) spectroscopies. The FTIR data show that cells cultivated in the presence of 0.2 mmol L⁻¹ of CuSO₄ produce larger amounts of pyruvated exopolissacharide (EPS) than the ones cultivated in its absence. The EPR data indicate that the amount of Cu²⁺ decreases with cultivation time. The ¹³C-CPMAS NMR data also show the complexation of Cu²⁺ ions to the EPS. The results demonstrate that EPS plays an important role in *Xac* Cu²⁺ protection. Both capsular and slime EPS act as an initial protection mechanism, binding free Cu²⁺ ions, reducing their diffusion and their active transport to the cytoplasm. Cu²⁺ also induces the production of a highly pyruvated negative EPS, increasing its capture and binding capacity.

Keywords: citrus canker, *X. axonopodis* pv. *citri*, exopolysaccharide, EPR, NMR, FTIR

Introduction

Xanthomonas axonopodis pv. *citri* (*Xac*) is the causal agent of citrus canker, a major problem in citriculture.[1,2] One of the methods to control the disease is the application of Cu²⁺ based bactericides, which reduce bacterial populations on plant surfaces.[1,3,4]

Copper is an essential element for all living organisms, but its excess is toxic to cells, inducing the formation of free radicals. As it is more toxic to lower organisms such as bacteria and fungi,[3] Cu²⁺ pesticides have been used in agriculture for over a century, to control plant diseases. This practice has selected copper resistant strains, reducing the efficacy of Cu²⁺ bactericides.[2]

Bacterial resistance has been reported in several phytopathogenic genera such as *Xanthomonas* and *Pseudomonas*, which infect hundreds of economically important plants.[3,5-7] Copper resistance has been reported in *Xanthomonas campestris* pv. *vesicatoria*, which infects pepper and tomato; *Xanthomonas campestris* pv. *juglandis*, a walnut pathogen; *Xanthomonas axonopodis* pv. *citri*, a citrus pathogen and *Pseudomonas syringae* pv. *tomato*, a tomato pathogen.[3,5,6]

The genetic basis for Cu²⁺ protection in gram-negative bacteria such as *Xac* is usually determined by the *cop* operon present in plasmid or in bacterial chromosome.[3,5,6] This operon contains four open reading frames (ORFs), *copA, B, C* and *D,* under the control of a copper inducible promoter, requiring the regulatory genes *copR* and *S*, coded immediately downstream of *copD*. Deletion and site direct

mutations in *P. syringae* pv. *tomato* suggest that *copA* and *copB* are essential for resistance and *copC* and *copD* are required for full resistance.[3,5,6]

A characteristic of the *Xanthomonas* genus is the copious production of exopolysaccharide (EPS), xanthan gum, released by the cells as slime in medium. The EPS is involved in cell protection, but its role in the protection mechanism against heavy metals is not well established. The xanthan gum is a 1,4 linked β-D-glucose polymer. Every alternated glucose contains a negative charged trisaccharide side chain with an internal mannose, glucuronic acid and a terminal mannose. The internal mannose can be acetylated in the O(6) position and the terminal one can be derived by a pyruvic acid moiety, joined by a ketal linkage in the O(4) and O(6) positions, leaving a free carboxylic acid group. The derivation of mannoses is dependent on species, environment (nutrients, pH and temperature) and age.[8]

In this paper we analyzed role of EPS in *Xac* Cu^{2+} resistance mechanism by Fourier transform infrared (FTIR), electron paramagnetic resonance (EPR) and nuclear magnetic resonance (NMR) spectroscopies. Our results show that both capsular and slime EPS play an important role in *Xac* Cu^{2+} protection mechanism. They act as an initial protection mechanism, binding free Cu^{2+} ions, reducing their diffusion and their active transport to the cytoplasm.

Experimental

Preparation of bacterial samples

The *Xanthomonas axonopodis* pv. *citri* (*Xac*) 306 strain isolated from citrus groves in São Paulo state, Brazil,[9] was used to study the EPS role in the Cu^{2+} resistance mechanism. The cells were cultivated in predefined M9 medium, at 28 °C in a rotary shaker. The *Xac* were also cultivated in M9 medium with 0.2 mmol L^{-1} of $CuSO_4$. The optical density of the cultures at 600 nm, 1 cm quartz cells, was monitored in a Shimadzu UV-Visible 1601PC spectrophotometer. The samples with optical density (OD) higher than 1 were diluted before the measurements.

After the interruption of the cultures, the cells were collected by centrifugation (4000 ×*g* for 20 min). The pellets were suspended in 0.5% NaCl solution and centrifuged twice. The final pellets were lyophilized and used for the FTIR, EPR and NMR analyses.

Fourier transform infrared spectroscopy (FTIR)

The FTIR spectra were acquired on a Paragon 1000 Perkin Elmer spectrometer, from 4000 to 400 cm^{-1}, 4 cm^{-1} of

spectral resolution and 64 scans. The samples were prepared in the form of KBr pellets, 1 mg of bacteria and 100 mg of KBr. The spectra were baseline corrected from 3000 to 2800 cm^{-1} and from 1800 to 900 cm^{-1} and normalized by the intensity of the amide II peak (intensity = 1) at 1550 cm^{-1}, which is related to biomass.[10,11]

Electron paramagnetic resonance spectroscopy (EPR)

The solid samples were analyzed by EPR spectroscopy using a Bruker EMX spectrometer (Bruker Biospin Corporation, Rheinstetten, Germany) operating in the X-band (9.8 GHz) with a spherical cavity, at 300 K. The relative intensity measurements were referenced by a ruby (Al_2O_3:Cr^{3+}) located in a fixed position inside the cavity below the sample. The g-factors were referenced by a MgO:Cr^{3+} (g = 1.9797) sample attached to the sample to be analyzed. The following experimental settings were used: microwave power 1 mW; modulation frequency 100 kHz; and modulation amplitude 0.2 mT. The WinEPR SimFonia[12] program was used to simulate EPR spectra.

Nuclear magnetic resonance spectroscopy (NMR)

Solid-state ^{13}C NMR spectra were acquired using a 9.4 T Varian Inova 400 spectrometer. The samples were compacted in a 5 mm zircon rotor. The CP/MAS (cross polarization/magic angle spinning) spectra of the samples spinning rate at 9 kHz were recorded with 4 μs pulse width, 13.4 ms acquisition time, 2.5 s of recycle time, and a 60 kHz decoupling field strength. All spectra were filtered by an exponentially decaying function (line broadening factor of 20 Hz).

Results and Discussion

Results

Figure 1 shows the optical density (OD) curves for the *Xac* cultures with and without Cu^{2+} as a function of the incubation time. The data are shown only up to the 3rd day to demonstrate the effect of Cu^{2+} at the beginning of the culture. Thereafter, the OD remained almost constant up to the end of the experiment (13 days).

The cells in M9 medium without Cu^{2+} showed a continuous growth from the beginning (log phase) up to the stationary phase in about 48 h. The cells cultivated in M9 medium with Cu^{2+} showed a reduction of OD values in the first 8 h, indicating cell death. After the adaptation period, the cells began to grow at a rate similar to the cells in the medium without Cu^{2+}. A similar lag time (12 h)

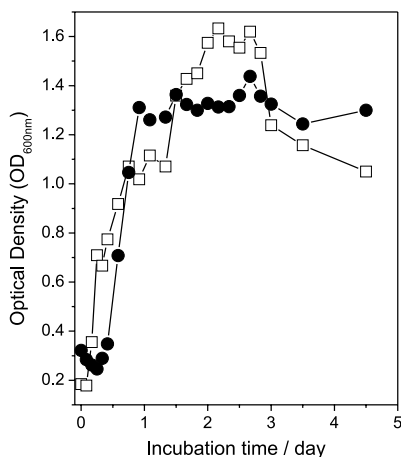was observed in the *X. campestris* pv. *vesicatoria copper* resistant strain.[7]

Figure 1. Optical density of *Xac* culture without (□) and with (●) 0.2 mmol L^{-1} of cupric sulfate.

The role of EPS in the *Xac* Cu^{2+} resistance mechanism was analyzed by FTIR, EPR and NMR spectroscopies.

FTIR analysis

Figure 2 shows the FTIR spectra of the *Xac* cells (2a) with its exopolisacharide and the exopolysaccharide, xanthan gum (2b), which is released into the medium as slime.
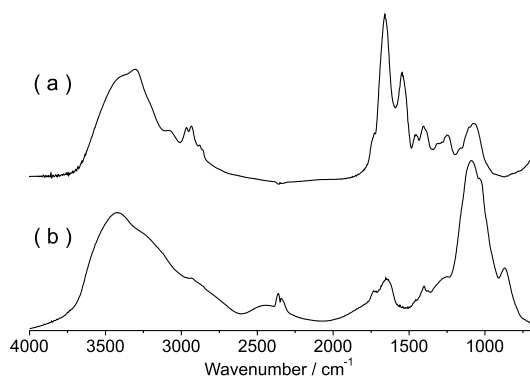

Figure 2. FTIR spectra of *Xac* (a) and xanthan gum (b).

Figure 2a is the *Xac* FTIR spectrum showing the major bands due to proteins, xanthan gum and lipids. The signals between 3600 and 3100 cm^{-1} are due to proteins and xanthan gum, N–H and O–H stretching; between 3000 and 2800 cm^{-1} due to C–H stretching of methyl and methylene groups; at 1730 cm^{-1}, due to C=O stretching of the xanthan acetate group (Figure 2b) and lipids; from 1700 and 1600 cm^{-1}, due to the proteins amide I band and to xanthan O–H angular deformation and to symmetric stretching

of carboxylate group of pyruvate and of glucuronic acid (Figure 2b); from 1700 to 1600 cm^{-1} due to protein amide II band, which is used as a internal standard for biomass content[10,11] and from 1100 and 900 cm^{-1} to xanthan C–O stretching (Figure 2b).

The xanthan gum FTIR spectrum (Figure 2b) also shows weak signals at 1400 cm^{-1} and at 1250 cm^{-1} due to carboxylate asymmetric stretching and to C=O acetate deformation, respectively.

Figure 3 shows some of the FTIR spectra (from 1800 to 900 cm^{-1}) of *Xac* incubated in M9 medium (3a) and in M9 medium with Cu^{2+} (3b). Figure 4 shows the variation of band intensity at 1730 cm^{-1}, 1640 cm^{-1}, and 1050 cm^{-1} for the spectra of Figure 3, due to acetate and pyruvate groups in xanthan and to the total xanthan, as a function of incubation time.

Figures 3a and 4a show small reduction in total xanthan content with incubation time. Figures 3b and 4b show a strong signal at 1640 cm^{-1} in 24 h. The intensities of signals at 1050 cm^{-1} and 1730 cm^{-1} were similar in both media and were constant with cultivation time, showing a slight increase in the cells cultivated in the presence of Cu^{2+} (4b); signal was constant with the cultivation time.
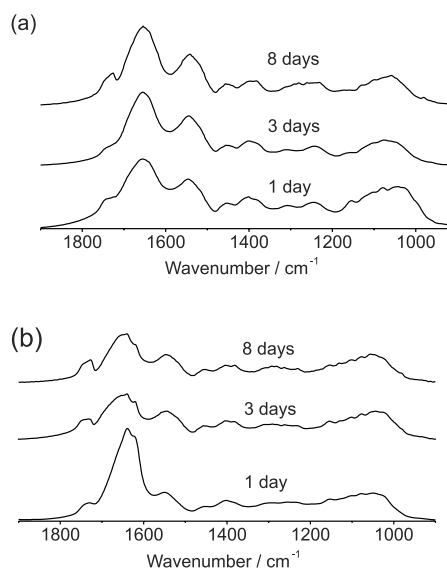

Figure 3. FTIR spectra of *Xac* for different incubation times. a) in M9 medium; b) in M9 medium with 0.2 mmol L^{-1} of cupric sulfate.

EPR analysis

The interaction of Cu^{2+} with *Xac* and xanthan gum was also analyzed by electron paramagnetic resonance spectroscopy (EPR). The EPR spectra of lyophilized *Xac* cultivated in M9 medium without Cu^{2+} (Figure 5a) show a broad line (ΔH *ca.* 600 G) that can be associated to Fe^{+3} in a ligand field with tetragonal symmetry.[13] The spectra after
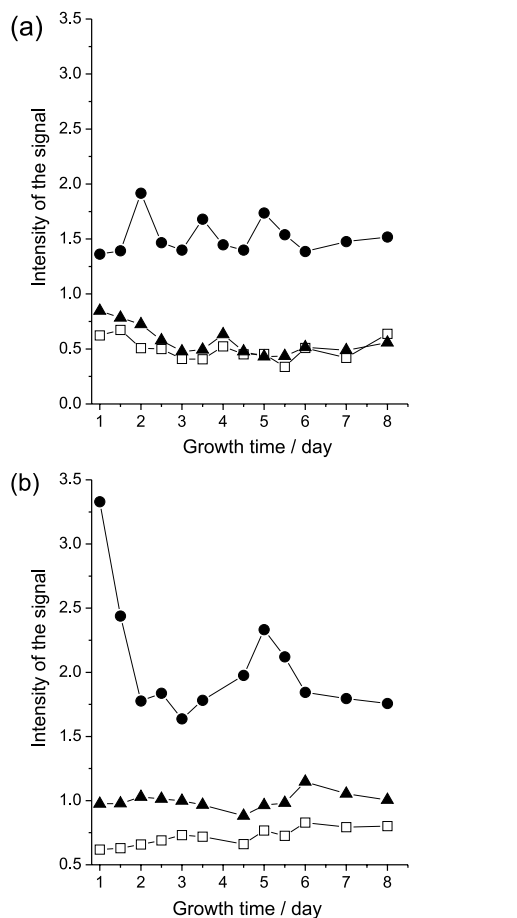
Figure 4. Normalized FTIR absorbance of the signals at 1730 (◆), 1640 (●), and 1050 cm^{-1} (□) from *Xac* cells for different incubation times in M9 medium (a) and in medium with 0.2 mmol L^{-1} of cupric sulfate (b).

5 days show a sharp line (ΔH *ca.* 10 G) at g = 2.00054, which is attributable to an unknown free radicals.[3]

Figure 5b shows some of the EPR spectra of lyophilized *Xac* cells obtained from the M9 medium with cupric sulfate. The spectra show only the typical signal of Cu^{2+} in an axial symmetric environment, with a 3d^9 electronic configuration and electronic spin S=1/2. The nuclear spin for both ^{63}Cu (natural abundance 69%) and ^{65}Cu (natural abundance 31%) isotopes is I=3/2. Therefore (2I+1), *i.e.*, four perpendicular and four parallel hyperfine components can be expected, resulting from the dipole-dipole interaction between the magnetic moment of the nucleus and the electronic moment of the paramagnetic ion. The spectra are axial type, having g//, g⊥ > 2, indicating the occupation of Cu^{2+} in an axial symmetry of a tetragonally distorted octahedral site.[13,14]

All the *Xac* EPR spectra (Figure 5b) were similar, showing a slight reduction in resolution with the incubation time. This suggests an increase of Cu^{2+} bound to cells, increasing the Cu^{2+}-Cu^{2+} dipolar interaction. Nakajima[14] showed that the Cu^{2+} spectral hyperfine structure was not observed only when the concentration in the cells exceed
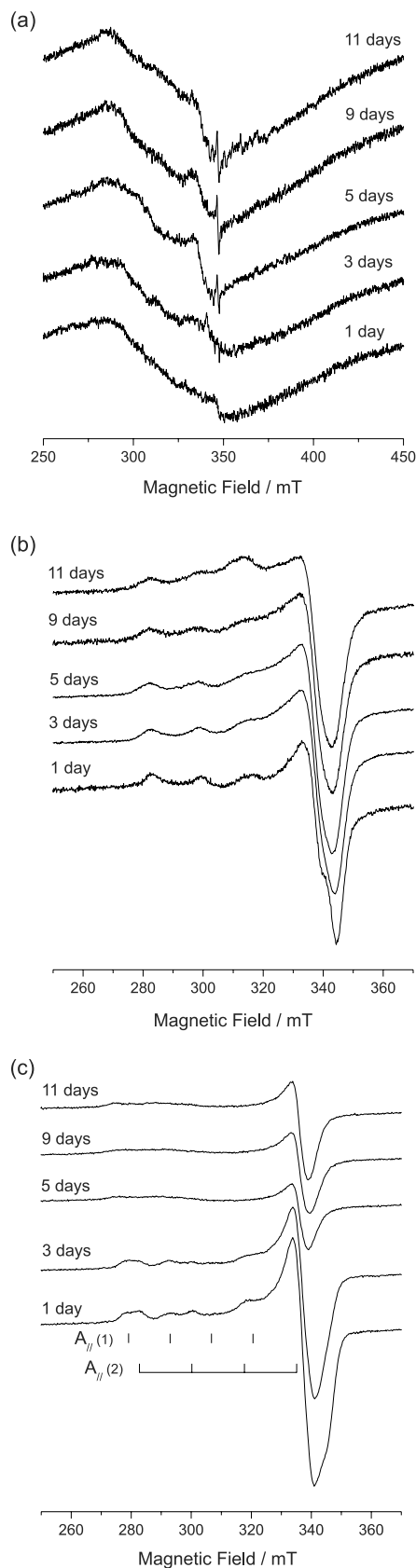

Figure 5. EPR spectra of *Xac* as a function of incubation times in M9 medium (a) and in M9 with cupric sulfate (b). EPR spectra of supernatant extracted from *Xac* cultures with cupric sulfate (c).

$400 \, \mu g \, g^{-1}$. This suggests that the Cu^{2+} concentrations in *Xac* samples were below this value. The EPR spectra in Figure 5b also show that the Cu^{2+} is bound in a similar environment, indicating no changes in the binding site in function of incubation time.

The EPR spectra of lyophilized supernatant, with the same mass (Figure 5c), show a continuous reduction of Cu^{2+} signals as a function of incubation time. The spectra of day 1 and 3 also show an overlap of Cu^{2+} signals in two distinct sites. Table 1 lists the $g_{//}$ and $g_{\perp}$ and $A_{//}$ values. In one site, Cu^{2+} spectra show similar parameters to the purified xanthan (Table 1) and the other to a Cu^{2+} complexed to the medium amino acids. Jung *et al.*[15] obtained values of $g_x = 2.038$, $g_y = 2.068$, $g_z = 2.390$ and $A_{//} = 13.5$ mT, which are similar to one of the measured supernatant values.

The supernatant spectra after day 3 showed only a broad line for $g_{//}$ signals. This type of reduction in resolution has also been observed for other bacteria and was also related to the pH below 4.[14] However, that was not the case here, since the media pH was always above 6. The spectra also show the reduction of Cu^{2+} in the medium, indicating its reduction or absorption by the bacteria.

Table 1. EPR spectra parameters of Cu(II) in *Xac*, xanthan gum and supernatant extracted from *Xac* cultures with cupric sulfate

Samples with Cu(II) ion	$g_{//}$	$g_{\perp}$
Xac	2.269	2.069
Xanthan gum	2.255	2.055
Supernatant - 3 days	2.260	2.055
	2.325	2.055
*Cu(Asn)+	2.390	$g_x = 2.038$
		$g_y = 2.068$

*Reference 15.

The values obtained for *Xac* and xanthan (Table 1) were similar to those obtained by Nakajima[14] for both gram-negative and gram-positive bacteria. Because the gram-negative and gram-positive bacteria have different cell wall components, he suggested that Cu^{2+} was sorbed by the surface proteins.

As the EPR spectra of *Xac* and xanthan are similar (Figure 5b and c, Table 1), showing identical environment, the Cu^{2+} have to be complexed preferentially with the OH and COO^- groups of xanthan, which is the major component of the *Xac* wall.

13C solid state NMR spectroscopy analysis

Figure 6 shows the high resolution solid state ^{13}C NMR spectra of *Xac* cells cultivated in M9 medium (6a) and M9 medium with Cu^{2+} (6b). The major signals in the NMR spectra can also be attributed to proteins and EPS as for FTIR (Figure 2). The strong signal at 175 ppm is due mainly to carbonyl carbons from proteins, fatty acids and EPS. The signals from 140 to 100 ppm were attributed to the aromatic amino acid side chains. The weak signal at 105 ppm is assigned to anomeric carbons of the glucose in xanthan and to C2 of the pyruvic acid ketal group. The strong signal at 75 ppm is assigned to the C2, C3 and C5 of the glucose polymer chain. The signals from 45 to 70 ppm were assigned to the α-carbon proteins and the signals from 15 to 45 ppm to aliphatic amino acid side chains, acetate and pyruvate methyl groups. The fatty acids signals were also detected by the stronger peak at 30 and 130 ppm, attributed to methylene groups and double-bound carbons, respectively. These signals overlapped with protein signals, but are well characterized in single pulse spectra (data not shown), similar to the ones observed in *Xylella fastidiosa*.[16]
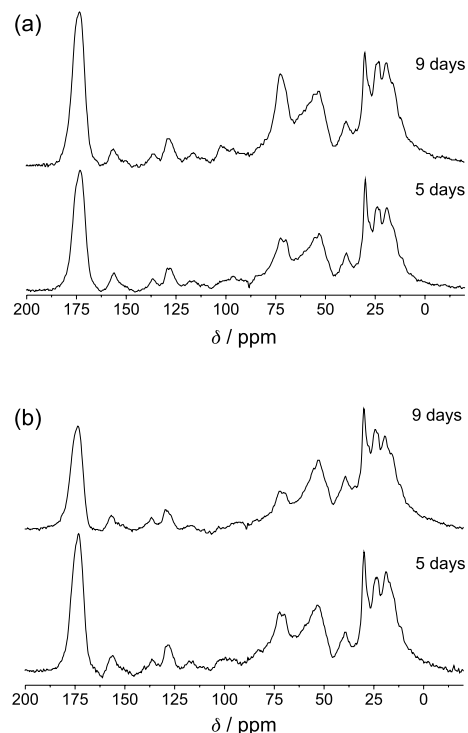

Figure 6. ^{13}C-CPMAS NMR spectra of *Xac* cell cultivated in M9 medium: without Cu^{2+} (a) and with Cu^{2+} (b).

The carbonyl peak at 175 and the EPS peak at 73 ppm for the cells cultivated without Cu^{2+} (Figure 6a) were stronger in 9 days than in 5 days, revealing a high capsular EPS in older cells. The spectra of cells cultivated with Cu^{2+} (Figure 6b) showed the opposite effect. The signals at 175 and 73 ppm were stronger in 5 days than in 9 days. These differences can be explained by the higher concentration of EPS and pyruvate groups in younger cultures and also by the effect of Cu^{2+} in longitudinal relaxation time of

the EPS carbons. As shown by EPR spectra, the Cu^{2+} are bound to capsular EPS in the carboxylate and OH groups. The EPS carbons that are closer to Cu^{2+} have a very short relaxation time, giving broad lines, and are not observed in the ^{13}C spectra.

A similar effect can be seen in the solid state ^{13}C NMR spectra of the xanthan gum extracted from the same cultures (Figure 7), where the ^{13}C signals for pyruvate and acetate C=O group are at 175 ppm and the CH_3 signals at 24 and 20 ppm, respectively. The signals from 85 and 55 ppm are attributed to carbons 2-6 of glucose, mannose and glucuronic acid. The signals from 105 to 95 ppm are due to quaternary C2 of the pyruvate and the C1-carbon of glucose, mannose and glucuronic acid. All the signals from the xanthan samples cultivated with Cu^{2+} show broader lines than the ones cultivated without it.
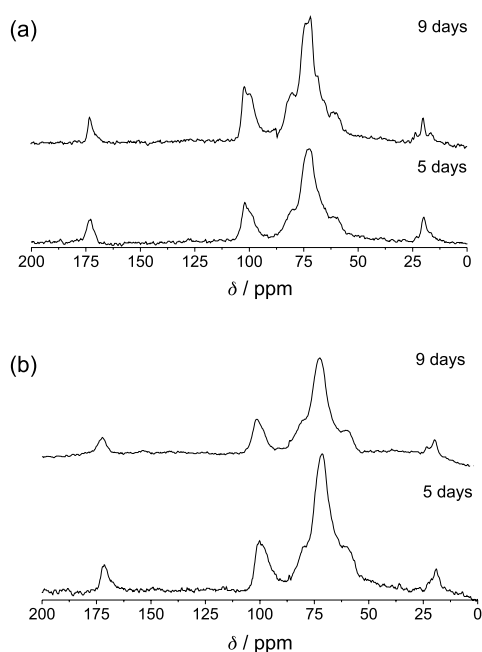

Figure 7. ^{13}C-CPMAS NMR spectra of xanthan gum extracted from *Xac* cultures in M9 medium (a), and in M9 medium with Cu^{2+} (b).

Conclusions

The FTIR, EPR and NMR spectroscopies show the variation of chemical composition in exopolysaccharide xanthan gum, in lyophilized *Xac* cultivated with and without of Cu^{+2} ions, in the media. The spectra show the toxic effect of Cu^{+2} ions, which has been used to control the citrus cancer disease in field, demonstrated by the increase of the EPS synthesis in the first stage of the culture.

As indicated in Figures 3 and 4, the cells cultivated in the presence of Cu^{2+} had a higher EPS content in all the fermentation times and displayed a very strong FTIR peak at 1640 cm^{-1}, indicating the presence of high carboxylate content. The extra carboxyl groups in the cells as due to overproduction of pyruvated EPS in response to Cu^{2+} ions. It is known that *Xanthomonas* can modulate the amount of acetate and pyruvate in its EPS as a function of nutrients, pH, temperature etc.[8]

The presence of more negative pyruvated EPS has a higher affinity to cations in the culture, increasing the rate of active cation transport as well as its binding capacity, as demonstrated by EPR and NMR data (Figures 5 to 7). The more negative pyruvated EPS produced by the cells in the first days of culture has stronger ability to harvest and bind the lethal Cu^{2+} ions in culture, keeping them outside the cells and not reaching the cytoplasm.

The xanthan gum produced as slime by the cells cultivated with Cu^{2+} was also more pyruvated in the initial days of culture (Figures 3 and 4). In addition to its harvesting and binding capacity, pyruvated xanthan also increased the culture viscosity, reducing cation diffusion.[8] The lower diffusion rate reduced the Cu^{2+} contact with cells, thus reducing its level in the cytoplasm.

A similar production of highly pyruvated xanthan has been observed when *Xanthomonas campestry* was treated with hypochlorous acid, which is known to induce free radicals such as Cu^{2+} ions. It has been demonstrated that the production of highly pyruvate xanthan is activated by the free radical inducible regulatory protein, SoxS, which binds DNA SoxS consensus sequence in the gum B promoter region, increasing the transcription of gum mRNAs.[17]

High expression of EPS has been reported as a response to Cu^{2+} ions in *Xylella fastidiosa,* which also causes Citrus disease and is related to *Xac*. The results also suggest a synergistic effect between diffusion barriers and other mechanisms associated with bacterial resistance in this phytopathogen.[18]

Xac cells seem to have a similar response to different lethal compounds, indicating that EPS is involved in a general and non-specific cell protection mechanism. Since EPS is continuously produced by the cells, *Xac* cells can be used in a fast protection mechanism, reducing the initial death rate and allowing for activation of specific protection mechanisms,[19] like *cop* operon, against Cu^{2+} ions. After this specific mechanism becomes effective, the production of highly pyruvated EPS is reduced to normal levels, as illustrated in Figures 3 and 4.

These data also indicate that Cu^{2+} based bactericides used in citrus canker control programs must be effective in the first application, as the cells with normal (low) pyruvated EPS, is not effective in protecting them against Cu^{2+}. If some cells survive the initial spraying, they are ready to face future applications with highly pyruvated EPS and with the copper operon activated, reducing the

effectiveness of Cu^{2+} bactericides or requiring application of higher Cu^{2+} doses.

Acknowledgments

References

1. del Campo, R.; Russi P.; Mara, P.; Mara, H.; Peyrou, M.; Ponce de Leon I.; Gaggero, C.; *FEMS Microbiol. Lett.* **2009**, *298*, 143.

2. Mendes, B. M. J.; Cardoso, S. C.; Boscariol-Camargo, R. L.; Cruz, R. B.; Mourão Filho, F. A. A.; Bergamin Filho, A.; *Plant Pathol.* **2010**, *59*, 68.

3. Cooksey, D. A.; *FEMS Microbiol. Rev*. **1994**, *14*, 381.

4. Graham, J. H.; Gottwald, T. R.; Cubero, J; Achor, D. S.; *Mol. Plant Pathol*. **1995**, *5*, 1.

5. Cooksey, D. A.; *Mol. Microbiol*. **1993**, *7*, 1.

6. Lee, Y. A.; Hendson, M.; Panopoulus, N. J.; Schroth, M. N.; *J. Bacteriol*. **1994**, *176*, 173.

7. Ramos, G. B. A; Rosato, Y. B.; *Braz. J. Genet*. **1996**, *19*, 551.

8. Casas, J. A.; Santos, V. E.; García-Ochoa, F.; *Enzyme Microb. Technol*. **2000**, *26*, 282.

9. da Silva, A. C. R.; Ferro, J. A.; Reinach, F. C.; Farah, C. S.; Furlan, L. R.; Quaggio, R. B.; Monteiro-Vitorello, C. B.; Van Sluys, M. A.; Almeida, N. F.; Alves, L. M. C.; do Amaral, A. M.; Bertolini, M. C.; Camargo, L. E. A.; Camarotte, G.; Cannavan, F.; Cardozo, J.; Chambergo, F.; Clapina, L. P.; Cicarelli, R. M. B.; Coutinho, L. L.; Cursino-Santos, J. R.; El-Dorry, H.; Faria, J. B.; Ferreira, A. J. S.; Ferreira, R. C. C.; Ferro, M. I. T.; Formighieri, E. F.; Franco, M. C.; Greggio, C. C.; Gruber, A.; Katsuyama, A. M.; Kishi, L. T.; Leite, R. P.; Lemos, E. G. M.; Lemos, M. V. F.; Locali, E. C.; Machado, M. A.; Madeira, A. M. B. N.; Martinez-Rossi, N. M.; Martins, E. C.; Meidanis, J.; Menck, C. F. M.; Miyaki, C. Y.; Moon, D. H.; Moreira, L. M.; Novo, M. T. M.; Okura, V. K.; Oliveira, M. C.; Oliveira, V. R.; Pereira, H. A.; Ross,i A; Sena, J. A. D.; Silva, C; de Souza, R. F.; Spinola, L .A. F.; Takita, M. A.; Tamura, R. E.; Teixeira, E. C.; Tezza, R. I. D.; dos Santos, M. T.; Truffi, D.; Tsai, S. M.; White, F. F.; Setubal, J. C.; Kitajima, J. P.; *Nature* **2002**, *417*, 459.

10. Naumann, D. In *Encyclopedia of Analytical Chemistry*; Meyers, R. A., ed., John Wiley & Sons: Chichester, UK, 2000, pp. 102-131.

11. Osiro, D.; Colnago, L .A.; Otoboni, A. M. M. B.; Lemos, E. G. M.; de Souza, A. A.; Coletta Filho, H. D.; Machado, M. A.; *FEMS Microbiol. Lett*. **2004**, *236*, 313.

12. Bruker Analytische Messtechnik GmbH; *WINEPR SimFonia shareware, Version 1.25*; Rheinstetten, Germany, 1996.

13. Griscom, D. L.; *J. Non-Cryst. Solids* **2004**, *40*, 211.

14. Nakajima, A.; *Water Res.* **2002**, *36*, 2091.

15. Jung, K.; Ristori, S.; Martini, G.; *Spectrochim. Acta, Part A* **2000**, *56*, 341.

16. Osiro, D.; Muniz, J. R. C.; Coletta Filho, H. D.; de Souza, A. A.; Machado, M. A.; Garratt, R. C.; Colnago, L.A.; *Biochem. Biophys. Res. Commun*. **2004**, *323*, 987.

17. Rao, Y. M.; Sureshkumar, G. K.; *Biotechnol. Bioeng.* **2001**, *72*, 62.

18. Rodrigues, C. M.; Takita, M. A.; Coletta-Filho, H. D.; Olivato, J. C.; Caserta, R.; Machado, M. A.; Souza, A. A.; *Appl. Microbiol. Biotechnol.* **2008**, *77*, 1145.

19. Chan, J. W. Y. F.; Goodwin, P. H.; *Biotechnol. Adv*. **1999**, *17*, 489.